The Inverse Gaussian Distribution in Wireless Channels: Second-Order Statistics and Channel Capacity

Imène Trigui, *Member, IEEE*, Amine Laourine, *Member, IEEE*, Sofiène Affes, *Senior Member, IEEE*, and Alex Stéphenne, *Senior Member, IEEE*

Abstract—In this paper, we introduce the Inverse Gaussian (IG) fading distribution to model the envelope and the power of the received signal in radio propagation fading channels and free-space optical (FSO) channels. The joint distribution of the IG process and its derivative and the marginal distribution of the derivative are developed. The obtained formulas are then used to derive the second-order statistics of the received signal envelope and the channel capacity under IG and Nakagami-IG (NIG) fading distributions. Numerical results sustaining our analysis are provided, and the impacts of various parameters on the system performance are investigated.

Index Terms—Composite fading distribution, FSO channels, inverse Gaussian (IG) distribution, Nakagami-IG (NIG) distribution, level crossing rate, average fade duration, channel capacity.

I. INTRODUCTION

EVEN after decades of research, the designers of future mobile communication systems are still aiming to identify, comprehend and analyze new tractable models to describe wireless fading channels. Fading models are typically used to fit the histogram of the empirical/experimental measurements of the envelope of the received random signals. Multipath fading is commonly modeled using the well-known Rayleigh, Weibull, Rice and Nakagami-m distributions. Recently, more generalized and flexible models, that can offer better fits to experimental data, have been proposed in [2] and [3]. On the other hand, shadowing phenomena are modeled by the well-known log-normal (LN) distribution (cf. [4] and references therein). However, there exist real situations, for which the LN distribution seems not to adequately fit the experimental data, although one or another may yield a moderate fitting. This is, for instance, accentuated for millimeter wave channels (60 GHz or above) with high human motion where the LN distribution failed in fitting the experimental measurements since the strong attenuation of the human body at 60 GHz considerably decreases the received power and changes the character of the fading statistics [5]. In addition, in free-space optical (FSO) communications, the atmospheric turbulence originating from inhomogeneous variations in temperature and

pressure increases the standard deviation of the shadowing amount on the channel fading the received signal is subjected to. Moreover, there exist analytical situations for which mathematical manipulations of the LN seems very cumbersome, although other distribution forms afford simplicity.

The facts above call for using an alternative tractable probability density function (pdf) to describe the physical problems at the origin of shadowing effects. As an alternative to overcome analysis intractability, researchers have employed the two-parameter Gamma distribution in place of the log-normal one [6]. This replacement, though yielding a closed form, fails to capture the tailed behavior of the log-normal distribution with large variance. Recently, the authors in [7]-[11] noticed that the inverse Gaussian (IG) distribution provided a better fit to the log-normal distribution. In addition to being tractable and similar to the log-normal distribution, the pdf of the inverse Gaussian shows a heavier tail relative to the LN [12] leading to the increase of the probability of the distribution at low amplitude values. The IG is therefore more adequate in allowing for a relatively higher shadowing level. This property may be suitable for channel measurements where there are several bodies with fast motion. By recalling the inverse Gaussian distribution, the authors of [7]-[11] aimed at providing closed-form expressions for the pdf, the error rates and channel capacity. However, these statistics do not provide any insight into the temporal behavior of the received signal. Thus, to cope with the high-data-rate requirements of new mobile communication systems, the analysis of the dynamic behavior of the channel is inevitable.

In this paper, the information pertaining to the fading behavior of the IG and the Nakagami-IG channels is obtained through the study of the Level Crossing Rate (LCR) and the Average Fade Duration (AFD) of both the envelope and the channel capacity. To this end, we derive an exact expression for the joint probability density of the IG process and its derivative, which, in contrast to many other distributions, are dependent. The obtained formulas are then employed to carry out a second-order analysis framework.

The rest of this paper is organized as follows. In Section II, we present the IG distribution and introduce its basic statistical parameters. Moreover, we provide an exact expression for the joint probability density of the IG process and its derivative. Using this new pdf, we provide in Section III closed-from expressions for the LCR and AFD of the envelope and the channel capacity under IG fading. In Section IV we consider the Nakagami-IG distribution as a compound model for composite fading shadowing environments and we study

its statistical properties for different levels of shadowing and fading. Finally, Section VII summarizes the main results and the conclusion of this work.

II. MARGINAL AND BIVARIATE PDF OF THE IG DISTRIBUTION

Let $\xi(t)$ be a stationary Inverse Gaussian random process (for short: $\xi \sim IG(\lambda, \beta)$) with the normalized underlying covariance function $\psi = \psi(\tau)$. The marginal and bivariate pdf of such a process are, respectively, given by [12]

$$p_\xi(y) = \sqrt{\frac{\lambda}{2\pi}} y^{-\frac{3}{2}} e^{\left(-\frac{\lambda(y-\beta)^2}{2\beta^2 y}\right)}, \quad y > 0. \qquad (1)$$

and

$$p_{\xi_1,\xi_2}(y_1, y_2) = \frac{\lambda}{4\pi} \sqrt{\frac{1}{(1-\psi^2)y_1^3 y_2^3}} \times$$
$$\left(e^{\frac{-\lambda}{2\beta^2(1-\psi^2)}\left(\frac{(y_1-\beta)^2}{y_1} + \frac{(y_2-\beta)^2}{y_2} - 2\psi\frac{(y_1-\beta)(y_2-\beta)}{\sqrt{y_1 y_2}}\right)} + \right.$$
$$\left. e^{\frac{-\lambda}{2\beta^2(1-\psi^2)}\left(\frac{(y_1-\beta)^2}{y_1} + \frac{(y_2-\beta)^2}{y_2} + 2\psi\frac{(y_1-\beta)(y_2-\beta)}{\sqrt{y_1 y_2}}\right)} \right). (2)$$

Note that, (2) is the latest bivariate extension of the IG distribution and that other forms of the joint distribution also exist [12]. The expectation and the variance of $\xi \sim IG(\lambda, \beta)$ are, respectively, given by λ and β^3/λ. Consequently, its coefficient of variation (CV) is given by $\sqrt{\beta/\lambda}$. Integration of (1) yields the Cumulative Distribution Function (CDF) expression of ξ given by

$$P_\xi(y) = \int_0^y p_\xi(y) dy = \frac{\beta\sqrt{\frac{\lambda}{2}}e^{\frac{\lambda}{\beta}}}{\pi} \int_0^{\frac{\lambda y}{2\beta^2}} y^{-\frac{3}{2}} e^{-y-\frac{\lambda^2}{4\beta^2 y}} dy$$
$$= \frac{\beta\sqrt{\frac{\lambda}{2}}e^{\frac{\lambda}{\beta}}}{\pi} \gamma\left(-\frac{1}{2}, \frac{\lambda y}{2\beta^2}, \frac{\lambda^2}{4\beta^2}, 1\right), \qquad (3)$$

where $\gamma(\cdot)$ is the is the generalized (lower) incomplete Gamma function [13, Eq. (6.1)]. An alternative expression for the CDF of ξ is given by

$$P_\xi(y) = N\left((y-\beta)\sqrt{\frac{\lambda}{\beta^2 y}}\right) + e^{\frac{2\lambda}{\beta}} N\left(-(y+\beta)\sqrt{\frac{\lambda}{\beta^2 y}}\right), \quad (4)$$

where $N(z)$ denotes the normal probability integral $N(z) = (2\pi)^{-1/2} \int_0^z e^{-1/2t^2} dt$ which can be evaluated by means of expansions such as given in [14].

In view of its versatile nature, the IG distribution has numerous applications in diverse fields [7]-[11] including wireless communications. In [8]-[10], the IG model was used for describing shadowing effects in RF wireless communications and shown to be an accurate substitute for the cumbersome log-normal distribution. Indeed, a comparison between these two probability density functions that was carried in [15] shows that when $CV \leq 1$, the two functions agree well. By recalling the following matching formulas between the two distributions

$$\lambda = \frac{e^\mu}{2\sinh(\frac{\sigma^2}{2})}, \quad \text{and} \quad \beta = e^{\mu + \frac{\sigma^2}{2}}, \qquad (5)$$

and considering the Loo's fading model introduced in [16], an urban area corresponds to $(\lambda = 1, \beta = 1)$ and a suburban area corresponds to $(\lambda = 30, \beta = 1)$. Note that, the condition $CV \leq 1$ is satisfied in both urban and suburban environments. When $CV > 1$, the inverse Gaussian density curve has a higher peak and a heavier tail compared to the log-normal density curve. Therefore, when early occurrences are dominant in the measured data distribution, the IG provides a suitable choice for the fading model. Though the log-normal distribution is also applicable in such cases, the IG presents the advantage of a closed-form mixture distribution.

In the context of optical systems, only recently have the authors of [11] considered the IG distribution for modeling turbulence-induced fading in FSO systems. All turbulence conditions considered in [11] verify $CV \leq 1$. Although being an interesting distribution with many applications, the IG model is still unknown namely in terms of its joint distribution $p_{\xi\dot\xi}(y, \dot y)$, where $\dot\xi(t)$ is the time derivative of the process $\xi(t)$. The latter can be derived by using the bivariate pdf $p_{\xi_1,\xi_2}(y_1, y_2)$ and the substitutions $y_1 = y - \tau\dot y/2$ and $y_2 = y + \tau\dot y/2$

$$p_{\xi\dot\xi}(y, \dot y) = \lim_{\tau\to 0} \tau p_{\xi_1,\xi_2}\left(y_1 = y - \frac{\tau\dot y}{2}, y_2 = y + \frac{\tau\dot y}{2}\right). \quad (6)$$

Recalling the McLauren series expansion of $\psi(\tau)$ and using the fact that for any real differentiable random process $\psi'(0) = 0$ [17], we have

$$\psi(\tau) \approx 1 + \frac{\psi''(0)\tau^2}{2} + O(\tau^3)$$
$$1 - \psi^2(\tau) \approx -\psi''(0)\tau^2 + O(\tau^3). \qquad (7)$$

By applying (7) to (2) and performing some manipulations, we obtain

$$p_{\xi_1,\xi_2}(y_1, y_2; \tau) \sim \frac{\lambda}{4\pi} \sqrt{\frac{1}{(1-\psi^2)y_1^3 y_2^3}} \times$$
$$e^{\frac{-\lambda}{2\beta^2(1-\psi^2)}\left(\left(\frac{(y_1-\beta)}{\sqrt{y_1}} - \frac{(y_2-\beta)}{\sqrt{y_2}}\right)^2 - \psi''(0)\tau^2 \frac{(y_1-\beta)(y_2-\beta)}{\sqrt{y_1 y_2}}\right)}. \quad (8)$$

Tacking into account (7) and resorting to the fact that

$$\lim_{\tau\to 0} \frac{\tau}{\sqrt{1-\psi^2}} = \sqrt{\frac{1}{-\psi''(0)}}, \qquad (9)$$

and

$$\lim_{\tau\to 0} y_1 = \lim_{\tau\to 0} y_2 = y, \qquad (10)$$

we obtain the joint pdf of ξ and $\dot\xi$ given by

$$p_{\xi,\dot\xi}(y, \dot y) = \lim_{\tau\to 0} \tau p_{\xi_1,\xi_2}\left(y_1 = y - \frac{\tau\dot y}{2}, y_2 = y + \frac{\tau\dot y}{2}\right)$$
$$= \frac{\lambda}{4\pi y^3 \sqrt{-\psi''(0)}} e^{-\frac{\lambda}{2\beta^2}\frac{\dot y^2}{-\psi''(0)y} - \frac{\lambda}{2\beta^2}\frac{(y-\beta)^2}{y}}. \quad (11)$$

From (11), it can clearly be seen that the joint pdf $p_{\xi,\dot\xi}(y, \dot y)$ cannot be written as a product of the marginal pdfs $p_\xi(y)$ and $p_{\dot\xi}(y)$. Hence, the processes $\xi(t)$ and $\dot\xi(t)$ are not statistically independent. Moreover, the distribution of the derivative $\dot\xi$ can
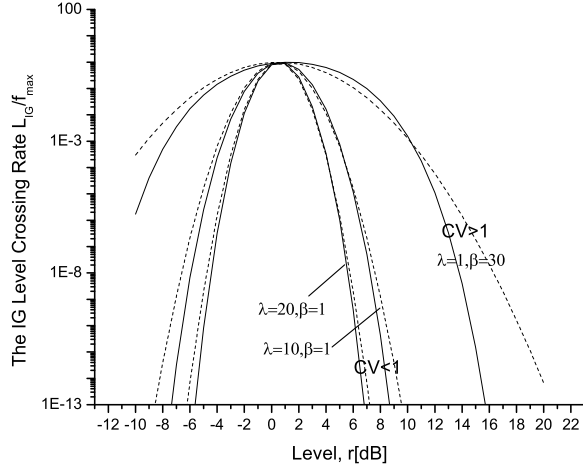
Fig. 1. Normalized LCR versus envelope level r in IG channels (continuous lines) and Lognormal channels (broken lines).

be obtained by integrating (11) over y as

$$
\begin{aligned}
p_{\dot{\xi}}(\dot{y}) &= \int_0^\infty p_{\xi,\dot{\xi}}(y,\dot{y}) dy \\
&= \frac{\lambda e^{\frac{\lambda}{\beta}}}{4\pi\sqrt{-\psi''(0)}} \int_0^\infty \frac{e^{-\frac{\lambda}{2\beta^2}\left(\frac{\dot{y}^2}{-\psi''(0)}+\beta^2\right)\frac{1}{y}-\frac{\lambda}{2\beta^2}y}}{y^3} dy.
\end{aligned}
\tag{12}
$$

The last integral can be calculated by the help of [18, Eq. (3.471.9)] as

$$
p_{\dot{\xi}}(\dot{y}) = \frac{\lambda e^{\frac{\lambda}{\beta}}}{2\pi\sqrt{-\psi''(0)}} \frac{K_2\left(\frac{\lambda}{\beta^2}\sqrt{\frac{\dot{y}^2}{-\psi''(0)}+\beta^2}\right)}{\left(\sqrt{\frac{\dot{y}^2}{-\psi''(0)}+\beta^2}\right)^2},
\tag{13}
$$

where $K_\lambda(\cdot)$ is the modified Bessel function of the second kind and order λ [18, Eq. (8.485)]. Moreover, the fractional moments of $\dot{\xi}$ can be easily obtained, for $k \in R^+$, as

$$
\begin{aligned}
m_k &= \mathrm{E}\left(\dot{\xi}^{2k}\right) = \int_{-\infty}^{+\infty} \dot{y}^{2k} p_{\dot{\xi}}(\dot{y}) d\dot{y} \\
&= \frac{(-\psi''(0))^k \Gamma\left(k+\frac{1}{2}\right)\left(2\beta^2\right)^{k-\frac{1}{2}}}{\pi\left(\frac{\lambda}{\beta}\right)^{k+\frac{1}{2}}} e^{\frac{\lambda}{\beta}} K_{k-\frac{3}{2}}\left(\frac{\lambda}{\beta}\right),
\end{aligned}
\tag{14}
$$

where $\mathrm{E}[\cdot]$ denotes the expectation operator.

III. LEVEL CROSSING RATE AND AVERAGE FADE DURATION

A. Inverse-Gaussian (IG) Channels

As an accurate and simple distribution that can efficiently model irradiance fluctuations in FSO systems, the IG channel has been addressed in [11] through its generalized moments and error probability. Here we provide the exact expressions for the LCR and the AFD for both the received signal envelope and the channel capacity.

The LCR of $\xi \sim IG(\lambda,\beta)$ at the level y, denoted by $L_{IG}(y)$ can be expressed, using [18, Eq. (3.461.3)], as

$$
L_{IG}(y) = \int_0^\infty \dot{y} p_{\xi,\dot{\xi}}(y,\dot{y}) d\dot{y} = \frac{\beta^2\sqrt{-\psi''(0)}}{4\pi y^2} e^{-\frac{\lambda}{2\beta^2}\frac{(y-\beta)^2}{y}}.
\tag{15}
$$

As a result, the average fade duration of $\xi \sim IG(\lambda,\beta)$ can be expressed as

$$
AF_{IG}(y) = \frac{P_\xi(y)}{L_{IG}(y)},
\tag{16}
$$

where $P_\xi(y)$ is the CFD of the IG process in (3). Then, by properly substituting (15) and (3) into (16), the AFD of $\xi \sim IG(\lambda,\beta)$ is obtained according to

$$
AF_{IG}(y) = \frac{4\sqrt{\lambda/2}y^2 e^{\frac{\lambda}{\beta}}}{\beta\sqrt{-\psi''(0)}} e^{\frac{\lambda}{2\beta^2}\frac{(y-\beta)^2}{y}} \gamma\left(-\frac{1}{2}, \frac{\lambda y}{2\beta^2}, \frac{\lambda^2}{4\beta^2}, 1\right).
\tag{17}
$$

Fig. 1 shows the LCR of $\xi \sim IG(\lambda,\beta)$ compared with the known log-normal LCR. It is clear that, for $CV \leq 1$, the IG LCR presented here provides a very good approximation of the log-normal LCR. As expected, when the CV is increased, this estimation becomes less robust until eventually the two distributions become completely divergent. The AFD of $\xi \sim IG(\lambda,\beta)$ is sketched in Fig. 2 for different values of the distribution parameters. We observe that increasing β results in the decrease of the AFD, meanwhile for higher values of λ, the AFD improves.

It is worth noting that similar results can be obtained for MIMO IG systems using a simple pure selection combining among L independent and identical brunches. By following the same reasoning of [19], we conclude that the LCR of the process $y = \max\{y_1, y_2, ..., y_L\}$ is the same as the LCR of any of the individual branches, i.e., it is given by equation (15). Moreover the CDF of y is given by

$$
P_L(y) = [P(y)]^L.
\tag{18}
$$

The statistical characterization of the IG channel can be done with the help of the mean, variance, pdf, and CDF and the LCR of the signal envelope. However, to cope with the high data rate requirements of new mobile communication systems, the analysis of the dynamic behavior of the channel capacity is inevitable. The instantaneous capacity of the IG channel $C(t)$ can be expressed as

$$
C(t) = \log_2(1 + SNR\xi(t)^2) \qquad \text{(bits/sec/Hertz)},
\tag{19}
$$

where SNR stands for the signal-to-noise-ratio.

The LCR $L_C(y)$ of the channel capacity $C(t)$ over IG channels is obtained as

$$
L_C(y) = \int_0^\infty \dot{y} p_{C,\dot{C}}(y,\dot{y}) d\dot{y},
\tag{20}
$$

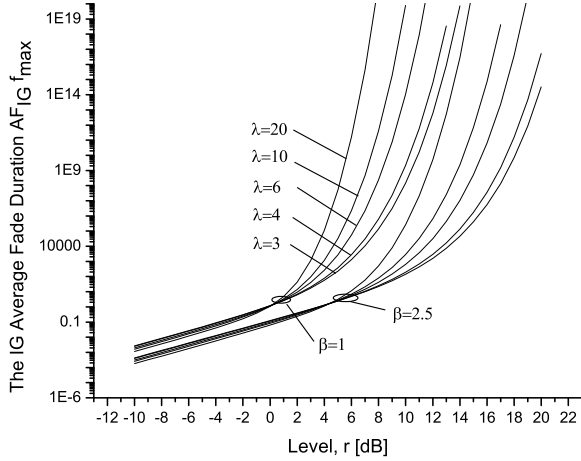where by applying the concept of transformation of random variables [17], we obtain

$$
p_{C,\dot{C}}(y,\dot{y}) = \left(\frac{2^y \ln(2)}{SNR}\right)^2 p_{\xi^2,\dot{\xi}^2}\left(\frac{2^y-1}{SNR}, \frac{2^y \dot{y} \ln(2)}{SNR}\right),
\tag{21}
$$

where $p_{\xi^2,\dot{\xi}^2}$ can be obtained using (11) as

$$
\begin{aligned}
p_{\xi^2,\dot{\xi}^2}(y,\dot{y}) &= \frac{1}{4y} p_{\xi,\dot{\xi}}(\sqrt{y}, \dot{y}/2\sqrt{y}) \\
&= \frac{\lambda e^{-\frac{\lambda}{8\beta^2}\frac{\dot{y}^2}{-\psi''(0)y^{\frac{3}{2}}} - \frac{\lambda}{2\beta^2}\frac{(\sqrt{y}-\beta)^2}{\sqrt{y}}}}{16\pi y^{\frac{5}{2}}\sqrt{-\psi''(0)}}.
\end{aligned}
\tag{22}
$$

Then, by properly substituting (22) and (21) into (20), and after some manipulations, a closed-form expression for the

Fig. 2.   Normalized envelope AFD versus envelope level r in IG channels.

Fig. 3.   Normalized capacity AFD versus the threshold level r in IG channels.

LCR of the capacity of the IG channel is shown to be given by

$$L_C(y) = \frac{\beta^2 SNR \sqrt{-\psi''(0)}}{4\pi(2^y - 1)} e^{-\frac{\lambda}{2\beta^2} \frac{\left(\sqrt{2^y-1} - \sqrt{SNR}\beta\right)^2}{\sqrt{SNR}\sqrt{2^y-1}}}. \quad (23)$$

The CDF $P_C(y)$ of the channel capacity $C(t)$ can be derived using (1) as follows

$$
\begin{aligned}
P_C(y) &= \frac{\ln(2)}{SNR} \int_0^y 2^x p_{\xi^2}\left(\frac{2^x - 1}{SNR}\right) dx \\
&= \frac{\ln(2)}{2}\sqrt{\frac{\lambda}{2\pi}} \int_0^y \frac{2^x}{2^x - 1} e^{-\frac{\lambda\left(\sqrt{\frac{2^x-1}{SNR}} - \beta\right)^2}{2\beta^2\sqrt{\frac{2^x-1}{SNR}}}} dx \\
&= \frac{\sqrt{2}\beta}{SNR^{3/2}}\left(\gamma\left(\frac{1}{2}, \frac{\lambda}{2\beta^2}\frac{\sqrt{2^y-1}}{\sqrt{SNR}}, \frac{\lambda^2}{4\beta^2}\right) + \right.\\
&\quad \left.\left(\frac{\lambda}{2\beta^2\sqrt{SNR}}\right)^2 \gamma\left(-\frac{3}{2}, \frac{\lambda}{2\beta^2}\frac{\sqrt{2^y-1}}{\sqrt{SNR}}, \frac{\lambda^2}{4\beta^2}\right)\right). \quad (24)
\end{aligned}
$$

Finally, the AFD of the channel capacity $C(t)$ under $\xi \sim IG(\lambda, \beta)$, denoted by $AFC_{IG}(y)$ can be obtained as
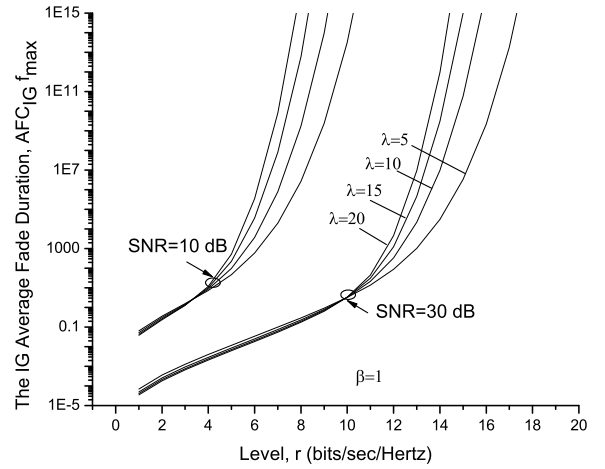
$$AFC_{IG}(y) = \frac{P_C(y)}{L_C(y)}, \quad (25)$$

where $L_C(y)$ and $P_C(y)$ are given by (23) and (24), respectively. In Fig. 3 we provide some numerical examples of the capacity AFD of the IG distributed channel. Here, we investigate the effect of the SNR and the distribution parameter λ with $\beta = 1$. As expected, the channel loses its impact on the capacity LCR by increasing the SNR. Moreover the channel becomes more severe by decreasing λ and hence the AFD performance deteriorates.

IV. COMPOUND-BASED IG CHANNELS

The Nakagami-IG (NIG) distribution arises from the product of two independent random processes

$$R(t) = \xi(t)\zeta(t), \quad (26)$$

where $\xi(t)$ is IG and $\sqrt{\zeta}$ is Nakagami-m distributed. The NIG includes the IG-Rayleigh and IG-exponential distributions as special cases. The resulting pdf of the NIG envelope $R(t)$ (for short: $R \sim NIG(\lambda, \beta, m, \Omega)$) is given by [10]

$$p_R(r) = Ar^{2m-1} \frac{K_{m+\frac{1}{2}}\left(\sqrt{\frac{2\lambda}{\beta^2}}\sqrt{mr^2 + \frac{\lambda}{2}}\right)}{\left(\sqrt{mr^2 + \frac{\lambda}{2}}\right)^{m+\frac{1}{2}}}, \quad (27)$$

where $A = \left(\sqrt{\frac{\lambda}{2\beta^2}}\right)^{m+\frac{1}{2}} \frac{\sqrt{\frac{\lambda}{2\pi}} 4m^m e^{\frac{\lambda}{\beta}}}{\Gamma(m)}$ and $m \geq 0.5$ is the Nakagami-m parameter. However, in our performance study, in order to derive closed-form expressions, we will restrict this parameter to integer values. Subsequently, for integer m, the CDF of $R \sim NIG(\lambda, \beta, m, \Omega)$ is shown to be given by

$$
\begin{aligned}
P_R(r) = 1 &- \frac{e^{\frac{\lambda}{\beta}} m^m \sqrt{\frac{\lambda}{\pi}}\left(\sqrt{\frac{\lambda}{\beta^2}}\right)^{m+0.5}}{(\sqrt{2})^{m-0.5}} \times \\
&\sum_{k=0}^m \frac{r^{2m-2k} K_{m-k-\frac{1}{2}}\left(\sqrt{\frac{2\lambda}{\beta^2}}\sqrt{mr^2 + \frac{\lambda}{2}}\right)}{\left(m\sqrt{\frac{\lambda}{2\beta^2}}\right)^k (m-k)! \left(\sqrt{mr^2 + \frac{\lambda}{2}}\right)^{m-k+\frac{1}{2}}}. (28)
\end{aligned}
$$

Proof: : see appendix.

The joint pdf $p_{\zeta, \dot\zeta}$ under Nakagami-m fading is given according to [4, Eqs. (2.20) and (9.721)] as

$$
\begin{aligned}
p_{\zeta, \dot\zeta}(x, \dot x) &= \frac{2\sqrt{2}m^{m+\frac{1}{2}}x^{2m-1}}{\sqrt{\pi}\Omega^{m+\frac{1}{2}}\Gamma(m)\sqrt{-\Delta''(0)}} e^{\left(-\frac{mx^2}{\Omega} - \frac{2m}{\Omega}\frac{\dot x^2}{-\Delta''(0)}\right)} \\
&\quad x > 0, m \geq 0.5, \quad (29)
\end{aligned}
$$

where $\Omega = E[\zeta^2]$ is the average power and $\Delta(\tau)$ is the normalized autocorrelation function (ACF) of $\zeta^2(t)$. For instance, the ACF under isotropic scattering conditions is [20]

$$\Delta(\tau) = 1 + J_0(2\pi f_\zeta) \quad \text{and} \quad -\Delta''(0) = (2\pi f_\zeta)^2, \quad (30)$$

where $J_0(\cdot)$ is the Bessel function of the first kind of order zero [18] and f_ζ denotes the maximum Doppler frequency shift influencing the multipath fading component.
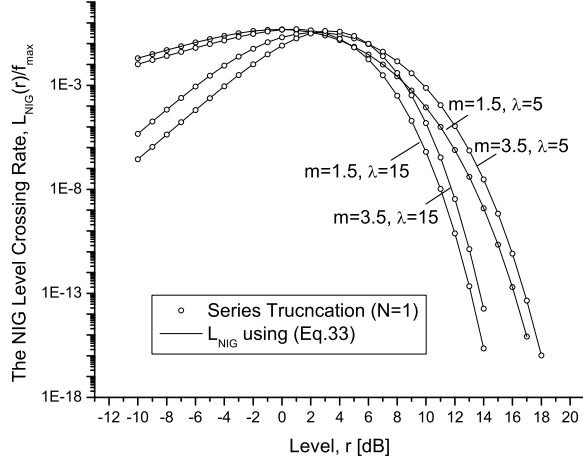
Fig. 4. Normalized LCR versus envelope level r in NIG fading channels, where the Doppler frequency shifts of the multipath and shadowing components of the fading are assumed $f_\zeta = 100 f_\xi$.

Referring to (26), when ξ and ζ are signal envelopes in some scattering fading channel subject to Doppler effect or to the turbulence effect originating from variations in the refractive index of the transmission channel in FSO channels, the signal envelopes ξ and ζ are time-correlated random processes and the LCR can be obtained according to [4, Eq. (9.725)] as

$$LCR(r) = \int_0^\infty \dot{r} p_{R\dot{R}}(r, \dot{r}) d\dot{r}, \qquad r \geq 0, \qquad (31)$$

where $p_{R\dot{R}}(r, \dot{r})$ is obtained according to

$$p_{R\dot{R}}(r, \dot{r}) = \int_0^\infty \frac{1}{y^2} \int_{-\infty}^{+\infty} p_{\zeta\dot{\zeta}}\left(\frac{r}{y}, \frac{\dot{r}}{y} - \frac{\dot{y}r}{y^2}\right) p_{\xi\dot{\xi}}(y, \dot{y}) d\dot{y} dy,$$
$$r \geq 0, \infty \leq \dot{r} \leq \infty. \qquad (32)$$

By properly substituting (11) and (29) into (31), the LCR of $R \sim NIG(\lambda, \beta, m, \Omega)$ at a level r, denoted by $L_{NIG}(r)$ can be expressed, using [18, Eq. (3.323.2)] and [18, Eq. (3.461.3)], as

$$L_{NIG}(r) = \frac{\sqrt{\lambda}\beta\sqrt{-\Delta''(0)}(\frac{m}{\Omega})^{m-\frac{1}{2}} e^{\frac{\lambda}{\beta}}}{4\pi\Gamma(m)} r^{2m-1}$$
$$\int_0^{+\infty} \frac{e^{-\frac{mr^2}{\Omega y^2} - \frac{\lambda}{2\beta^2}y - \frac{\lambda}{2y}}}{y^{2m+3}} \sqrt{y^3 + \frac{-\psi''(0)4m\beta^2 r^2}{-\Delta''(0)\Omega}} dy. (33)$$

It is important to mention that the above integral can be computed numerically with any desired accuracy by using Matlab or Mathematica. Distinctively, by using the Taylor series expansion

$$\sqrt{1+x} = \sum_{n=0}^\infty \binom{1/2}{n} \left(x^n \theta(1-x) + x^{\frac{1}{2}-n}\theta(x-1)\right),$$
$$(34)$$

where $\theta(\cdot)$ is the Heaviside's theta (unit) function [18], and performing some algebraic manipulations, (33) can be converted into the sum of two incomplete integrals converging

very fast, that is,

$$L_{NIG}(r) = \frac{\sqrt{\lambda}\beta^2\sqrt{-\Delta''(0)}(\frac{m}{\Omega})^m e^{\frac{\lambda}{\beta}} r^{2m}}{2\pi\Gamma(m)} \sum_{n=0}^\infty \binom{1/2}{n}$$
$$\left(Q_{-n}(r)\int_0^{Q_{1/3}(r)} y^{3n-2m-3} e^{-\frac{mr^2}{\Omega y^2} - \frac{\lambda}{2\beta^2}y - \frac{\lambda}{2y}} dy + \right.$$
$$\left. Q_{n-\frac{1}{2}}(r)\int_{Q_{1/3}(r)}^\infty y^{-3n-2m-\frac{3}{2}} e^{-\frac{mr^2}{\Omega y^2} - \frac{\lambda}{2\beta^2}y - \frac{\lambda}{2y}} dy \right), (35)$$

where $Q_n(r) = \left(\frac{-\psi''(0)4m\beta^2 r^2}{-\Delta''(0)\Omega}\right)^n$. It is worth noting that the LCR given in (35) converges rapidly. Indeed, the choice $N = 1$ is enough for an approximation as it can be shown in Fig. 4. Eventually, after substituting [13, Eqs. (6.1) and (6.2)] into (35), the LCR under NIG can be readily obtained as

$$L_{NIG}(r) \approx \frac{\sqrt{\lambda}\beta^2\sqrt{-\Delta''(0)}(\frac{m}{\Omega})^m e^{\frac{\lambda}{\beta}} r^{2m}}{2\pi\Gamma(m)} \sum_{k=0}^\infty \frac{(-\beta^2)^k}{k!}$$
$$\left(Q_0(r)\gamma\left(P_0 - k - 2, \frac{\lambda}{2\beta^2}Q_{1/3}(r), \frac{mr^2}{2}\frac{\lambda}{2\beta^2}, 2\right) + \right.$$
$$Q_{-\frac{1}{2}}(r)\Gamma\left(P_0 - k - \frac{1}{2}, \frac{\lambda}{2\beta^2}Q_{1/3}(r), \frac{mr^2}{2}\frac{\lambda}{2\beta^2}, 2\right) +$$
$$\frac{Q_{-1}(r)}{2}\gamma\left(P_{-1} - k - 2, \frac{\lambda}{2\beta^2}Q_{1/3}(r), \frac{mr^2}{2}\frac{\lambda}{2\beta^2}, 2\right) +$$
$$\left.\frac{Q_{\frac{1}{2}}(r)}{2}\Gamma\left(P_1 - k - \frac{1}{2}, \frac{\lambda}{2\beta^2}Q_{1/3}(r), \frac{mr^2}{2}\frac{\lambda}{2\beta^2}, 2\right)\right), (36)$$

where $P_n = 3n - 2m$. Note that even though this expression seems more complicated than (33), it can be very useful in the analysis of several LCR properties, namely the asymptotic ones.

Finally, substituting (33) and (28) into (16), one can readily obtain the AFD of the received envelope $R \sim NIG(\lambda, \beta, m, \Omega)$ at a threshold r.

Some numerical examples of the LCR and the ADF of $R \sim NIG(\lambda, \beta, m, \Omega)$ for different fading environments, (i.e., for different values of m) are presented in Figs. 4, 5 and 6 where the parameter Ω for Nakagami-m distribution was set to be equal to $2m$. All these results are analyzed for urban ($\lambda = 1, \beta = 1$) and suburban ($\lambda = 30, \beta = 1$) environments. It is quite obvious form Fig. 5 that the parameter m has a prominent effect on the statistics of the NIG channels. For low signal levels r, the LCR of channels with low values of m is higher than that of channels with higher values of m. While for high signal levels r, the LCR of channels with low values of m is lower than that of channels with higher values of m. Moreover, it can be observed that decreasing the value of the shadowing parameter λ increases the spread of the LCR of the channel envelope, while it decreases the maximum value of the LCR. Hence, when the shadowing and multipath fading figures $\{m, \Omega\}$ and/or λ, β increase, the LCR decreases as expected. Also from Fig. 4, it is observed that the curve with $(m = 1.5, \lambda = 5)$ has the same slope as the curve with $(m = 3.5, \lambda = 5)$, in contrast to the curve with $(m = 1.5, \lambda = 3.5)$ who has a steeper slope. This implies that a stronger shadowing dominates the LCR performance.
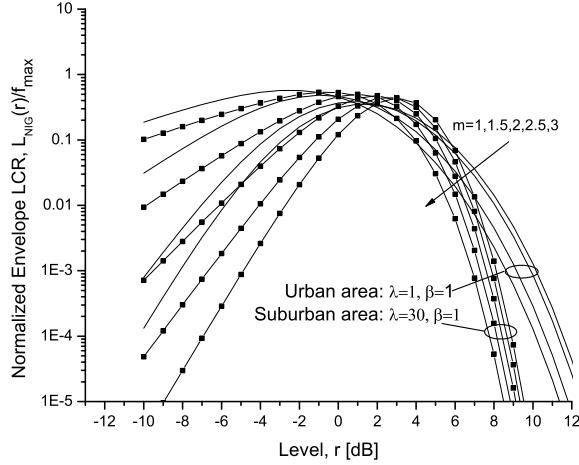
Fig. 5. Normalized LCR versus envelope level r in NIG fading channels, where the Doppler frequency shifts of the multipath and shadowing components of the fading are assumed $f_\zeta = 100 f_\xi$.

Fig. 6. Normalized AFD versus envelope level r in NIG fading channels, where the Doppler frequency shifts of the multipath and shadowing components of the fading are assumed $f_\zeta = 100 f_\xi$.

Similarly, the same statement is true for the envelope AFD as shown in Fig. 6.

By following the same rationale used to obtain the LCR of the capacity under IG distributed channels, the LCR of $C(t)$ under NIG channels can be readily expressed as

$$LC_{NIG}(r) = \frac{\sqrt{\lambda}\beta\sqrt{-\Delta''(0)}(\frac{m}{SNR\Omega})^{m-\frac{1}{2}}e^{\frac{\lambda}{\beta}}(2^r-1)^{m-0.5}}{16\pi\Gamma(m)} \times$$
$$\int_0^{+\infty} \frac{1}{y^{2m+3}} e^{-\frac{m(2^r-1)}{\Omega y^2 SNR} - \frac{\lambda}{2\beta^2}y - \frac{\lambda}{2y}} \times$$
$$\sqrt{y^3 + \frac{-\psi''(0)4m\beta^2(2^r-1)}{-\Delta''(0)\Omega SNR}} dy. \quad (37)$$

Using the concept of transformation of random variables, the pdf $p_C(y)$ of the channel capacity $C(t)$ can be found as

$$p_C(r) = \frac{2^r \ln(2)}{SNR} p_{R^2}\left(\frac{2^r-1}{SNR}\right)$$
$$= A\frac{2^r \ln(2)}{SNR^m}(2^r-1)^{m-1} \times$$
$$\frac{K_{m+\frac{1}{2}}\left(\sqrt{\frac{2\lambda}{\theta^2}}\sqrt{\frac{m}{SNR}(2^r-1)+\frac{\lambda}{2}}\right)}{\left(\sqrt{\frac{m}{SNR}(2^r-1)+\frac{\lambda}{2}}\right)^{m+\frac{1}{2}}}. \quad (38)$$

Moreover, the CDF $P_C(y)$ of the NIG channel capacity $C(t)$ can be obtained as follows

$$P_C(r) = \frac{A}{2}SNR\left(1 - J_{m,m+1}\left(\sqrt{\frac{2^r-1}{SNR}}, m+1, \frac{\lambda}{2}\right)\right) +$$
$$\frac{A}{2}\left\{1 - J_{m,m}\left(\sqrt{\frac{2^r-1}{SNR}}, m, \frac{\lambda}{2}\right)\right\}, \quad (39)$$

where $J_{p,q}(x, y, z)$ is given in (43). Consequently, the AFD expression of the capacity under $NIG(\lambda, \beta, m, \Omega)$ is the ratio between (37) and (39). In Figs. 7 and 8 we show some curves of the capacity LCR and AFD under NIG channels. From
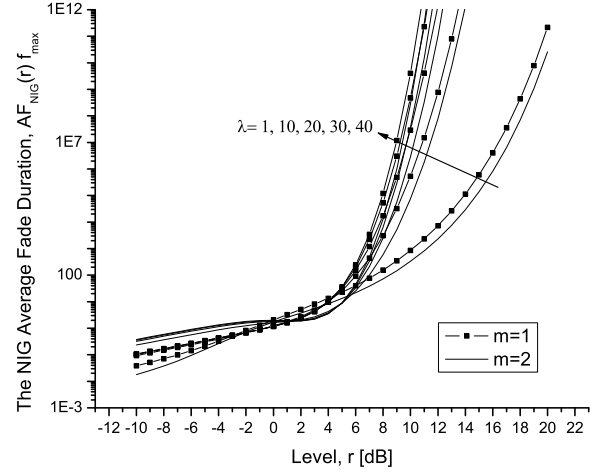

Fig. 7. Normalized LCR of the capacity versus threshold level r in NIG fading channels, where the Doppler frequency shifts of the multipath and shadowing components of the fading are assumed $f_\zeta = 100 f_\xi$.
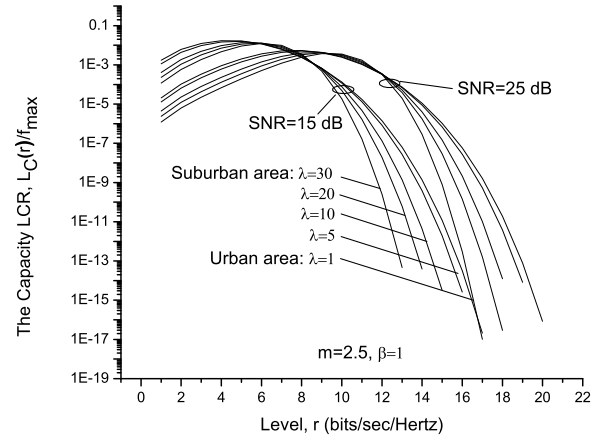
Fig. 7, we observe that increasing the shadowing standard deviation (small λ) decreases the maximum value of the LCR of the channel capacity, while it obviously increases the spread of the IG pdf. From Fig. 8, it can be observed that, for low signal levels r, the AFD of the channel capacity at low values of m is lower than that of channels with higher values of m. While for high signal levels r, the AFD of the channel capacity at low values of m is higher than that of channels with higher values of m.

V. CONCLUSION

Drawing upon the classical crossing theory of random processes, we have derived new closed-from formulas for the second-order statistics of inverse Gaussian distributed channels. We have derived analytical expressions for the CDF, LCR, and ADF of the envelope and channel capacity of the IG and the mixture IG channels. Moreover, we have
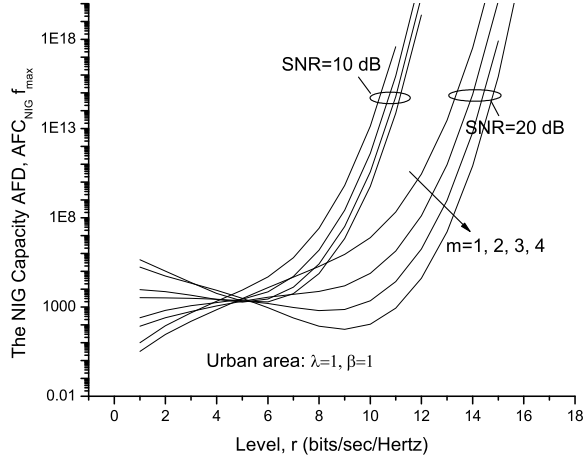
Fig. 8. Normalized AFD of the capacity versus threshold level r in NIG fading channels, where the Doppler frequency shifts of the multipath and shadowing components of the fading are assumed $f_\zeta = 100 f_\xi$.

investigated the effect of the distribution parameters, that reflect the shadowing and fading severity in the context of RF communications and the turbulence strength in the context of FSO, on the obtained metrics. The results presented in this paper are quite useful for the design and analysis of land mobile terrestrial channels.

VI. APPENDIX: CUMULATIVE DISTRIBUTION FUNCTION (CDF) OF NIG

The CDF of the received $R \sim NIG(\lambda, \beta, m, \Omega)$ is obtained upon integration of (27) as

$$P(r) = \frac{A}{2} \left[J_{m,m} \left(r^2, m, \frac{\lambda}{2} \right) - J_{m,m} \left(0, m, \frac{\lambda}{2} \right) \right], \quad (40)$$

where

$$J_{p,q}(x,y,z) = \int x^{q-1} \frac{K_{p+\frac{1}{2}}(b\sqrt{xy+z})}{(\sqrt{xy+z})^{p+\frac{1}{2}}} dx, \quad (41)$$

and $b = \sqrt{\frac{2\lambda}{\beta^2}}$.
Using the fact that

$$\frac{dx^{-s}K_s(x)}{dx} = -x^{-s}K_{s+1}(x), \quad (42)$$

and integrating by parts (41), we obtain

$$J_{p,q}(x,y,z) = -(q-1)! \sum_{k=0}^{q} \frac{2^k x^{q-k}}{(yb)^k (q-k)!}$$
$$\frac{K_{p-k+\frac{1}{2}}(b\sqrt{xy+z})}{(\sqrt{xy+z})^{p-k+\frac{1}{2}}}. \quad (43)$$

Using (43), the CDF of the received envelope $R \sim$

$NIG(\lambda, \beta, m, \Omega)$ can be readily obtained as

$$P(r) = 1 - \frac{e^{\frac{\lambda}{\beta}} m^m \sqrt{\frac{\lambda}{\pi}} \left(\sqrt{\frac{\lambda}{\theta^2}} \right)^{m+0.5}}{(\sqrt{2})^{m-0.5}}$$

$$\sum_{k=0}^{m} \frac{2^k r^{2m-2k}}{\left(m\sqrt{\frac{2\lambda}{\theta^2}} \right)^k (m-k)!} \frac{K_{m-k-\frac{1}{2}} \left(\sqrt{\frac{2\lambda}{\theta^2}} \sqrt{mr^2 + \frac{\lambda}{2}} \right)}{\left(\sqrt{mr^2 + \frac{\lambda}{2}} \right)^{m-k+\frac{1}{2}}}. \quad (44)$$

REFERENCES

[1] I. Trigui, A. Laourine, S. Affes, and A. Stéphenne, "On the level crossing rate and average fade duration of composite multipath/shadowing channels," in *Proc. 2008 IEEE Globecom*.

[2] M. D. Yacoub, "The κ-μ distribution and the η-μ distribution," *IEEE Antennas Propag. Mag.*, vol. 49, no. 1, pp. 68–81, Feb. 2007.

[3] M. D. Yacoub, "The α-μ distribution: a physical fading model for the Stacy distribution," *IEEE Trans. Veh. Technol.*, vol. 56, no. 1, pp. 27–34, Jan. 2007.

[4] M. K. Simon and M.-S. Alouini, *Digital Communication over Fading Channels,* 2nd edition. Wiley, 2004.

[5] S. Collonge, G. Zaharia, and G. E. Zein, "Influence of the human activity on wide-band characteristics of the 60 GHz indoor radio channel," *IEEE Trans. Wireless Commun.*, vol. 3, no. 6, pp. 2396–2406, Nov. 2004.

[6] P. M. Shankar, "Performance analysis of diversity combining algorithms in shadowed fading channels," *IEEE Wireless Pers. Commun.*, no. 1–2, pp. 61–72, Apr. 2006.

[7] R. Agrawal and B. Karmeshu, "Ultrasonic backscattering in tissue: characterization through Nakagami-generalized inverse Gaussian distribution," *Computers Biology Med.*, vol. 37, pp. 166–172, 2006.

[8] B. Karmeshu and R. Agrawal, "On efficacy of Rayleigh-inverse Gaussian distribution over K-distribution for wireless fading channels," *Wireless Commun. Mobile Computing,* vol. 7, no. 1, pp. 1–7, Jan. 2007.

[9] T. Eltoft, "The Rician inverse Gaussian distribution: a new model for non-Rayleigh signal amplitude statistics," *IEEE Trans. Image Process.*, vol. 14, no. 11, pp. 1722–1735, Nov. 2005.

[10] A. Laourine, M.-S Alouini, S. Affes, and A. Stéphenne, "On the performance analysis of composite multipath/shadowing channels using the G-distribution," *IEEE Trans. Commun.*, vol. 57, no. 4, pp. 1162–1170, Apr. 2009.

[11] N. D. Chatzidiamantis, H. G. Sandalidis, G. K. Karagiannidis, and M. Matthaiou, "Inverse Gaussian modeling of turbulence-induced fading in free-space optical systems," *J. Lightwave Technol.*, vol. 29, no. 10, May 2011.

[12] R. S. Chhikara and L. Folks, *The Inverse Gaussian Distribution: Theory, Methodology, and Applications*. M. Dekker, 1989.

[13] M. A. Chaudhry and S. M. Zubair, "On a class of incomplete Gamma functions with applications," 2002.

[14] M. Abramowitz and I. A. Stegun, *Handbook of Mathematical Functions with Formulas, Graphs, and Mathematical Tables*, 9th edition. Dover Publications, 1972.

[15] K. Takagi, S. Kumagai, I. Matsunagaf, and Y. Kusaka, "Application of inverse Gaussian distribution to occupational exposure data," *Ann. Accup. Hyg.*, vol. 41, no. 5, pp. 505–514, 1997.

[16] C. Loo, "A statistical model for a land mobile satellite link," *IEEE Trans. Veh. Technol.*, vol. 34, pp. 122–127, 1985.

[17] A. Papoulis, *Probability, Random Variables, and Stochastic Processes*, 3rd edition. McGraw-Hill, 1991.

[18] I. S. Gradshteyn and I. M. Ryzhik, *Table of Integrals, Series and Products,* 7th edition. Academic, 1994.

[19] M. D. Yacoub, J. E. V. Bautista, and L. G. de Rezende Guedes, "On higher order statistics of the Nakagami-m distribution," *IEEE Trans. Veh. Technol.*, vol. 48, no. 3, pp. 790–794, May 1999.

[20] T. Tjhung and C. Chai, "Fade statistics in Nakagami-lognormal channels," *IEEE Trans. Commun.,* vol. 47, no. 12, pp. 1769–1772, Dec. 1999.